Article

Surface/interface carrier transport modulation for constructing photon-alternative ultraviolet detectors based on self-bending assembled ZnO nanowires

Zhen Guo, Lianqun Zhou, Yuguo Tang, Lin Li, Zhiqi Zhang, Hongbo Yang, Hanbin Ma, Arokia Nathan, and Dongxu Zhao

ACS Appl. Mater. Interfaces, **Just Accepted Manuscript** • DOI: 10.1021/acsami.7b08066 • Publication Date (Web): 17 Aug 2017

Surface/interface carrier transport modulation for constructing photon-alternative ultraviolet detectors based on self-bending assembled ZnO nanowires

Zhen Guo,[1] Lianqun Zhou,[1] Yuguo Tang,[1] Lin Li,[2] Zhiqi Zhang,[1] Hongbo Yang,[1] Hanbin Ma,[3] Arokia Nathan[3] and Dongxu Zhao[4*]*

1.Key Lab of Bio-Medical Diagnostics, Suzhou Institute of Biomedical Engineering and Technology, Chinese Academy of Sciences. No.88，Keling Road, Suzhou New District, 215163, People's Republic of China E-mail: guozhen@sibet.ac.cn; zhaodx@ciomp.ac.cn;

2.Key Laboratory for Photonic and Electronic Bandgap Materials, Ministry of Education, School of Physics and Electronic Engineering, Harbin Normal University, Harbin 150025, PR China.

3.Department of Engineering, University of Cambridge, Cambridge CB3 0FA, UK

4.The State Key Laboratory of Luminescence and Applications, Changchun Institute of Optics, Fine Mechanics and Physics, Chinese Academy of Sciences, 3888 East Nan-Hu Road, Open Economic Zone, Changchun 130033, People's Republic of China

KEYWORDS (Surface/interface; carrier control; UV photodetection; self-bending assembly; ZnO nanowires)

ABSTRACT Surface/interface charge carrier generation, diffusion and recombination/transport modulation are especially important in the construction of photodetectors with high-efficiency in the field of nanoscience. In the paper, a kind of ultraviolet (UV) detector is designed based on ZnO nanostructures considering photon-trapping, surface plasmonic resonance (SPR), piezophototronic effect, interface carrier trapping/transport control and collection. Through carefully optimized surface/interface carrier transport modulation, the designed device with detectivity as high as of 1.69×10^{16} / 1.71×10^{16} cm·Hz$^{1/2}$ /W irradiating with 380 nm photons

under ultralow bias of 0.2V are realized by alternating nanoparticle/nanowire active layers, respectively, and the designed UV photodetectors shows a fast and a slow recovery processes of 0.27 ms and 4.52 ms, which well satisfy paractical needs. In further, it is observed that UV photodetection could be performed within alternative response under varying correlated key parameters, through efficient surface/interface carrier transport modulation, spectrally resolved photoresponse of the detector revealed controlled detection in the UV region based on the ZnO nanomaterial, photodetection is allowed or limited by varying active layers, irradiation distance from one of the electrodes, standing states or electric field. The detailed carrier generation, diffusion, recombination/transport processes are well illustrated to explain charge carrier dynamics contributing to the photoresponse behaviors.

1. INTRODUCTION

Charge carrier generation, diffusion and recombination modulation are all very important considerations in the construction of high-efficiency light-emitting diodes, photodetectors and solar cells in the field of optoelectronic devices. [1-5] The surface or interface properties of nanomaterials are especially significant to the overall charge carrier generation, transport, recombination and/or collection efficiency because the reaction dynamics can be greatly influenced by these properties.[6-9] In the case of applications involving photodetection with high performance, semiconductor nanoparticles and nanowires could be conjugated taking advantage of their merits. However, they both have advantages and disadvantages with respect to their photoelectric characteristics. Nanocrystal particles exhibit strong photon absorption productivity for generating carriers in the extended bands, resulting in efficient carrier collection.[10,11] However, a photoelectric device with a channel layer composed of nanoparticles can exhibit

unfavorable carrier transport of the generated carriers; the surface/interface-traps-modulated hopping and tunneling processes dominate the performance of such devices.[12,13] The photodetectors based on thin films of semiconductor nanocrystal particles demonstrate remarkably high responsivities accompanied with slow responses; meanwhile, large driving voltages are commonly requested. [14] To achieve high gain and low dark current, a large electrode spacing (>5 mm) is needed to allow more photons to be absorbed; and the transit time of the charges across the electrodes is correspondingly increased, and the applications of these photodetectors are thus limited.[14-17] By contrast, semiconductor nanowires possess ideal transport characteristics with optimal carrier mobility, exhibiting non-negligible dark current.[18,19] Therefore, during the past decade, nanowire-based ultraviolet photodetectors have been widely explored, with most efforts focusing on single nanowires or arrays because their merits of high crystal quality and facile fabrication make them suitable for fabricating optoelectronic devices. However, for several reasons, ultraviolet photodetector devices based on nanoparticles or nanowires have not shown comparative advantages. Epitaxial single-crystal nanowires have almost no grain boundaries, exhibit much better optoelectronic performances when used in related devices because of the greater carrier diffusion length (>175 μm in single-crystal nanowires, more than two orders of magnitude longer than the diffusion length in nanocrystalline thin films), and have a low trap-state density; indeed, a nearly 100% internal quantum efficiency has been achieved in single-crystal nanowire solar cells.[3,20] The photogenerated carriers in single crystals can be completely extracted because of the long carrier diffusion length when the active layer thickness is much larger than that of the thin film, which is highly applicable in photodetection fields. As such, methods to combine the advantages of nanocrystal particles with many grain boundaries and a high density of charge-carrier traps and the advantages of

nanowires with excellent crystal quality for carrier transport with high mobility have been developed; efforts to enable good control of charge-carrier transport and trap limitation for building high-efficiency optoelectronic devices are becoming a research hot spot. The issue on how to design photodetectors with low dark current, high detectivity and quick response utilizing nanoparticle and nanowire structures remains a key challenge. Here, in contrast to these previously reported photodetectors, we developed an ultraviolet detector with modulated photoresponse by exploring a vertical structure that combines the low-dark-current noise of nanoparticles and the high mobility of single crystalline nanowires with adjustable standing states. The active layer material composed of a free standing or self-bending assembly ZnO nanowires and nanoparticles is emerging as a highly applicable nanomaterial because of its high exciton binding energy (60 meV) and wide bandgap (3.4 eV) at room temperature.[14,21] ZnO is considered as a low-cost material; it can be prepared by various synthetic strategies and has potential applications in optoelectronic devices.[15,22-24] The preparation of carrier collection electrodes with ZnO nanowires homoepitaxially grown on a nanoparticle film results in a photoactive layer composed of a ZnO nanocrystal particle film with a thickness of 50 nm and epitaxial single-crystal nanowires longer than 5 μm; these active layers are sufficiently thick for almost all the ultraviolet photons to be completely absorbed. Additionally, to take advantage of the high gain of the photoconductors, at least one of the electrodes is required to be an ohmic contact. ZnO nanowires with free or bending states, when employed as the photoabsorber layer and as high-carrier-mobility electrodes on a ZnO nanoparticle film, can outperform earlier photodetectors because of the application of its nature of ZnO material. Given the piezophototronic effect of ZnO, a vertical-structured photodetector that combines the advantages of nanoparticles and nanowires could be efficiently modified through the design of epitaxial

nanowires with changing-standing-states carrier trapping or transport behaviors,[25-27] such modification would result in a photodetector with alternative photoresponse, the spectrally resolved photoresponses of the detector reveal photoselective detection in the ultraviolet region, which could be well modulated by the photosensitive region, location, electric field and standing states of the nanowires. The specific ultraviolet detectivity as high as of 1.69×10^{16} / 1.71×10^{16} cm·Hz$^{1/2}$ /W when illuminated from different locations is realized considering photon trapping, surface plasmon resonance and piezophototronic effects together. Because of the competition of the surface/interface-charge transport and recombination modulation of the generated carriers, the photoresponse characteristics under different conditions could be well illustrated by the detailed carrier generation, recombination and diffusion mechanisms, combining the energy band diagram and charge carrier dynamics for the contribution of the photoresponse behaviors.

2. RESULTS AND DISCUSSION

ZnO nanoparticles with different size of 60, 30 and 15 nm repectively were firstly prepared on quartz glass by magnetron sputtering method for obtaining controlled growth of nanowires as shown in Fig.1(a-c), by exploring solution process ZnO nanowires can be prepared assisted with nanoparticle seed layer in a large scale as shown in the top scanning electron microscopy (SEM) images in Fig.1(d-o), which indicate that the standing states could be well adjusted via changing the growth conditions, as discussed in the materials preparation section, non-bended, less bended and heavily bended ZnO nanowires with tops aggregated together could be formed by exploring different supporting nanoparticles, through seed size adjustment of the ZnO nanoparticles, the geometry of the epitaxial nanowires could be efficiently tunned, the aspect ratio for the obtained nanowires could be 38, 63 and 102, finally the posture of the epitaxial nanowires from vertically aligned to less bended or heavily bended were completely transformed as shown in the figure,

which proves seed size plays an important role in tunning the aspect ratio of the nanowires to enable the formation of different standing states by solution process. Considering photoelectric device fabrication utilizing ZnO nanoparticles and nanowires with controlled morphology, which both function as essential photoactive and/or efficient carrier-transport/trapping layers, combining energy band and nano size engineering, it is believed that corresponding built devices performance could be efficiently improved. Here, a schematic diagram of our ultraviolet photodetector is presented as shown in Fig. S1, (the corresponding prepare precedure was shown in Fig. S2) which explores free standing or self-bending assembled ZnO nanowires on a nanoparticle layer as photoactive layer supported by a quartz glass substrate. Experimental results demonstrate that the ultraviolet absorption spectrum was further broadened through the combination of ZnO nanoparticles and nanowires (Fig. S3), the higher-energy ultraviolet photons could be efficiently absorbed as a result of the quantum size effect.[28]

As show in Fig.2(a-l), a kind of UV photodetector was designed by considering the key factors such as photon trapping, ZnO-Au SPR reasonance, piezophototronic effects and energy band engineering. Firstly, the self-bending assembled ZnO nanowires mimic the pyramid texture, similar to the anti-reflection layer of Si solar cells as shown in SEM image from top view (Figs.2b,c,S4),[29,30] a pyramidal surface texture that causes photon trapping by scattering light into the sensitive region over a large angular range in conventional thick Si solar cells has been demonstrated to be very efficient for increasing the absorption coefficient in solar cell applications (Fig.2c).[30] Self-bending assembled ZnO nanowires have long absorption path lengths for photon trapping, especially in high-density nanowire arrays, resulting in carrier collection or transport for efficient carrier extraction.[19] The self-bending-state nanowires with their tops aggregated together increase the effective path length in the framework structure; these

nanowires have been demonstrated to be an excellent material for efficient photon trapping, especially in the UV region over a large angular range. Secondly, to both minimize the dark current and increase the photocurrent, Au nanoparticles were functionalized on the surfaces of the nanoparticles and nanowires. The carriers near the surface of ZnO nanostructures can thus be depleted, and the width of the depletion layer is increased.[31] As surface plasmon resonance has been determined to lead to a strong absorption, scattering and local field enhancement when the size of plasmonic Au-ZnO nanostructures is less than the incident wavelength, which results in improved UV photodetection. [32] [23,32,] [16] In the present work, through modification of Au nanoparticles on the surfaces of the ZnO nanostructures, the absorption spectrum is broadened into the visible region, accompanied by enhanced UV intensity, as shown in Fig.S3. SEM image of Au nanoparticles could be well applied for surface modification of ZnO nanowires as shown in Fig.2e. The high resolution trasmission electron microscopy (HRTEM) image displays the lattice fringes of the Au/ZnO nanostructure interface, from which the interplanar spacing was measured to be 0.260 and 0.235 nm for the ZnO (002) and Au (111) planes shown in Fig.2f, respectively. Surface plasmon resonance could be applied here for lowering dark current meanwhile improving photocurrent as shown in energy band diagram between Au and ZnO materials (Figs.2d, S5). Thirdly, As we know, piezophototronic effects could be applied for improving performance of the photoelectric devices through energy band structure modification as shown in Fig.2g, [33-35] as shown in Fig.2g, capilary force induced self-bending assembly of ZnO nanowires with tops aggregated together can thus applying piezophototronic effects for wurtizite structure. The TEM image of the nanowires shows small size variation with an average diameter of ~60 nm (Fig.2i). The detailed TEM image indicates that the tops of the epitaxial nanowires exhibit a nanoneedle-like shape. Meanwhile, in the case of single nanowire, a uniform

size distribution from the root to the neck is observed. The HRTEM image shows that the single-crystal nanowires have lattice fringes perpendicular to the wire axis, which indicates that the epitaxial nanowires grew along the [0001] direction. The equal interplanar distance measured along the nanowire was 2.60Å, which means that lattice parameter *c* is uniform along the whole nanowire in both the free-standing and bent states. Finally, considering quantum size effect, the photongenerated carriers in nanoparticles owning larger band gap compared with nanowires could be easily diffused into nanowires as shown in the schematic energy band diagram in Fig. 2(j), otherwize, there is a barrier layer for blocking carrier transport from nanowires to nanoparticles unless optimal electric filed is loaded. TEM images of the ZnO nanowires with nanoparticles or dispersed ZnO nanoparticles as seed layer for the growth of the homoepitaxial nanowires was captured in Fig. 2(k,l), which demonstrates uniform size distribution of nanowires and nanoparticles, and the homo-epitaxial growth mode of the c-axis oriented ZnO nanowires was supported by the same oriented nanocrystal particles.

Interestingly, the photonalternative response shown in Fig.3(a-i) was observed in the photocurrent spectra for the detector under UV illumination of 380 nm on self-bending assembled ZnO nanowires (assigned as the top side) and quartz glass (assigned as the bottom side). A peak appeared at approximately ~380 nm in the photocurrent spectrum when irradiated from the top side; this peak is attributed to the nearby band edge response. The full-width at half-maximum (FWHM) of the photoresponse spectrum is ~34 nm, which means that the response of the photodetector to the photons is limited in a certain spectral range. When the UV irradiation was focused on the bottom side, a new peak appeared at ~350 nm in the shorter-wavelength region. This peak is attributed to the higher energy absorption-related photoresponse due to the presence of high energy states.[36] The self-bending assembled ZnO nanowire photodetector works

as follows: firstly, both the active layers of the nanoparticle film and nanowires absorb incident photons and generate photocarriers when illuminated from the bottom with ultraviolet light. The excited ZnO nanoparticles inject electrons across the nanoparticle/nanowire interface. The ZnO nanowires then provide the photon-injected carriers with a direct pathway to the collection region. While the photodetector is irradiated from the top side, more carriers are generated in the nanowires than in the nanoparticle film, and restricted charge transport over the grain boundaries of the nanoparticles limits the effective carrier collection. Because of the efficient carrier trapping among ZnO nanoparticles, the carrier transport properties of these systems are thus strongly limited in the dark. Under UV photon excitation, considering energy band diagram of nanowires and nanoparticles, the generated carriers in nanoparticles could be easily diffused into nanowires, otherwise, there is a barrier layer for blocking carrier transport from nanowires to nanoparticles unless optimal electric filed is loaded. Nonlinear increases in the free carrier density for the nanoparticle/nanowires irradiated with different wavelengths results in the current becoming strongly interface limited. This observed characteristic indicates that the proposed photodetector has potential applications in detecting photons with energies within a certain range. The highly selective response mechanisms can be also understood as follows: In the ZnO nanowire/nanoparticle structure, two regions exist in the active layer of the photodetector: a depletion region on the outerlayer and a neutral region below the surface. Because a proportional correlation exists between the penetration length and the wavelength, the photons whose energy is greater than the bandgap of ZnO (3.35 eV) will be efficiently absorbed by the depletion region. Nevertheless, under a smaller electric field in the neutral region, the main part of the photogenerated charge carriers cannot reach the depletion region during their lifetime; thus, the photoresponse signal becomes weaker. As a result, the higher-energy photons will be filtered by

the neutral region, making the photodetectors highly spectrum-selective.[37] As shown in Fig.3(b,c), the photocurrent spectra of the as-grown and gold-nanoparticle-decorated ZnO nanostructures demonstrate that surface modification can remarkably improve the performance of the photodetectors when irradiated on the top or bottom side, respectively, it could be noted that similar spectra shapes maitained with increasing photocurrent intensity under same conditions, which demonstrates the photoselective detection behavior was not changed. Here, a model based on energy band theory is proposed here to provide a better understanding of the enhancement mechanisms as shown in Fig.S5. In the dark, a depletion layer with low conductivity is created near the surface of ZnO by adsorbed oxygen molecules capturing the free electrons on the ZnO surface, and the surface states strongly depend on the Au nanoparticle coverage because of the further increased surface-to-volume ratio after surface modification. Additionally, the materials have different work functions (Au: 5.1eV; ZnO: 4.1 eV),[38] and the same Fermi energy levels, the charge carriers near the surface of ZnO are depleted by the negatively charged Au nanoparticles, the formation of the increased depletion region is one of the key reasons for decreasing the dark current.[31] Under UV irradiation, the negatively charged oxygen ions are discharged with the photogenerated holes through surface charge-carrier recombination, the conductivity of the ZnO device was increased by these photogenerated electrons. Because of hole trapping, the formed barrier at the Au/ZnO interface allows more electrons to be collected. Therefore, the interfaces and the particle-induced scattering for increased light absorption efficiency are responsible for the enhancement of the photoresponse.[39] As shown in Fig. 3(d-f), the mechanism of photoselective detection in the ZnO nanostructured photodetector by measuring the photocurrent with local irradiation of a light spot at different distance from one of the electrodes, where light irradiation was focused from the top side. The

photogenerated carriers were diffused along the bent nanowires, resulting in a weak photocurrent signal when illuminated at the midpoint between electrodes. When the light spot was close enough to one of the electrodes, the generated carriers had sufficient energy to cross the interface barrier via tunneling or thermal emission, resulting in an enhanced shorter-UV-wavelength photoresponse signal for decreasing surface recombination. While the active layer was irradiated in the depletion region or at a location less than a diffusion length away, the local electric field quickly swept away photogenerated electrons and holes in opposite directions from the region. Therefore, the recombination rate was greatly depressed, which greatly enhanced the local conductance. Moreover, the local net charge density in the depletion layer was reduced through the migration of the generated carriers. Thus, the local electric field was weakened, resulting in an enhanced photocurrent in the shorter-UV-wavelength region. Through data fitting analysis, the photocurrent located at 300, 320 and 350 nm shows exponetial decay with decay distance factor of ~107 μm^{-1} when changing irradiation distance from one of the electrodes. As shown in Fig.3(g-i), the strong local electric field quickly swept away the photon-generated carriers from the depletion region at a location less than a diffusion length away, which resulted in a reduced height of the interface barrier for increasing the migration of carriers into the metal electrodes.[40] However, because of the high recombination rate, the contribution of efficiently collected charge carriers for increasing photocurrent in the center region between the electrodes became much weaker. The electric field dependence of the photocurrent near the electrode contacts varied such that the currents were dominated by electric-field-induced carrier separation. Under larger electrical fields, the trapped carriers with higher migration energy will become free with increasing photocurrent. When the electric field was increased from 92.3 to 461.5 V/cm, a shorter-wavelength-region band photocurrent from 300 to 350 nm was enhanced, which

demonstrates the shorter wavelength-response recovery phenomenon under a stronger electric field (Fi.g 3e) is realized. The dependent of the photocurrent on the electric field and the photoactive layers enable photoselective detection, the transition of the shorter-UV-wavelength response from low to high was accompanied by a switch of the electric field, reflecting the influence of the majority carrier concentration on the photogenerated carrier recombination rates. The electric field-dependent photocurrent labeled at 380 and 350 nm exhibited exponential growth with growth constant factor of 418 and 191 cm/v, respectively, which demonstrates efficient carrier injection and collection in the designed ZnO nanostructure photodetector especially under larger electric field. Meanwhile, considering the influence factors such as active layer morphology for resulting in the decrease of shorter UV wavelength photocurrent, corresponding experiments were carried out for exploring detailed response mechanisms utilizing free standing ZnO nanowires for designing photodetectors as shown in Fig. S6, enhanced photocurrent could be realized based on self-bending assembled ZnO nanowire photodetector, here, the specific ratio was designed as SR:

$$SR = P_{\lambda 1} / P_{\lambda 2}, \qquad 1)$$

where P_{λ} represents photocurrent under certain wavelength irradiation, it could be clearly observed that much larger SR could be realized for self-bending assembled ZnO nanowire photodetector while the photocurrent at shorter wavelength range from 300 to 350 nm matains in the same level. Experimental results demonstrate that photogenerated carriers could be efficiently collected by the electrodes especially at the shorter UV wavelength, which could be realized as generally observed in the literatures. [23,41] As a piezoelectric material, charge carriers could be trapped by the bending-strain-induced piezopotential, which induced a substantial

change in the conductivity of the ZnO nanowires. Because of the polarization of ions, a piezoelectric potential is created in the crystal with noncentral symmetry under bent state. Hence, the charge transport is tuned by piezopotential, and a channel is created by the local piezoelectric charges via band modification at the interface region.[40,42] For the self-bending-assembled ZnO nanowires, the strain in the wire was mainly axial compressive strain given the capilary-force-induced bending state, in accordance with the studies by Wang et al, the responsivity of the photodetector under compressive strain could be enhanced more than several folds by introducing strain, notably, the direction of the *c*-axis of the ZnO will influence the photodetection signal based on single nanowire devices placed in-plane.[42] In our design, vertically aligned ZnO nanowires preferred the (002) *c*-axis orientation and the generated piezopotential could not switch signs.[40,42]

It is speculated that almost of the photogenerated carriers could be efficiently collected by electrodes under UV irradiation of different wavelength on the bottom side based on the experimental results and energy band diagram of nanowires and nanoparticles in the above, here, I-V characteristics were carriered out for the ZnO nanostructure photodetectors as shown in Fig. 4 (a-i), the *I-V* measurements of the self-bending-assembled ZnO nanowire photodetector devices were carried out without and with Au-nanoparticle modification. Under UV illumination with photon energy is greater than the bandgap of ZnO, the photocurrent increased greatly compared with the dark current (Fig.4b-d). Because of the local surface plasmon resonance caused by the Au nanoparticles on the surface of the ZnO nanostructures, the dark current decreased and the photocurrent increased, as shown in Fig.4c. The photocurrent for the Au-nanoparticle modified photodetector increased greatly especially under irradiation wavelength of 380 nm, which could be due to higher near band edge absorption for contributing photocurrent.

Photoexcitation with photon energies greater than the band gap of ZnO could be applied for generating carriers by the higher energy levels, however, due to the mechanisms discussed in accordance as mentioned in the above, the photocurrent becomes a little weaker.[43,44] When the photodetector was irradiated with ultraviolet light at a certain position, strong local carrier injection was induced in the area surrounding the light-absorbing ZnO material because of band modification caused by the electric field in the local environment.[14,40] Electrons in ZnO's valence band will be excited into the conduction band under the irradiation of photons with energies greater than the band gap, leaving holes in the valence band. Photocurrent is thus produced by these photon-generated carriers only when they can be efficiently collected by the electrode before recombination occurs. Under top side UV irradiation with photon energies greater than the bandgap of ZnO, the drifting process should dominate the transport of the carriers because of an external electric field. Because the external electric field across the nanowire-nanoparticle detector is mainly distributed in the depletion region, photogenerated carriers inside the active layer, especially those generated by the shorter UV wavelengths, are not efficiently collected by the electric field unless the minority carrier diffusion length is large. A strong competition between carrier recombination and diffusion processes dominates the overall performance of the nanoparticle-nanowire photodetector under different wavelengths for the contribution of nonlinear I-V characteristics. Due to the efficient carrier trapping in the nanostructral device, the dark current of the photodetector under an ultralow driven bias of 0.2 V was as low as 0.7 nA as shown in Fig. 4d, fast increase of the photocurrent as high as 10 μA is realized under UV irradiation of 380 nm with the same bias. The responsitivity can be expressed as:

$$R_\lambda = (I_\lambda - I_d) / P_\lambda S , \qquad 2)$$

where I_λ presents the photocurrent, I_d presents the darkcurrent, P_λ presents photocurrent, and S presents effective irradiation area, the caculated R_λ =~2.605×10^{5}A/W (0.2V), which is an ultra-high value obtained under such a very low bias, in other word, a low-cost, high sensitivity UV detector is designed. According to equation:

$$R_\lambda = q\lambda\eta G / hc , \qquad 3)$$

where q is elemental charge, λ is the incident wavelength, η is the quantum efficiency, if η=1, the phton gain can be: G=8.5×10^5,

and the obtained detectivity for top side irradiation could be expressed as:

$$D_T = R_\lambda / (2qJ_d)^{1/2} \qquad 4)$$

the caculated detectivity for the top side irradiation could be: D_T =1.69 × 10^{16} cm·Hz$^{1/2}$ /W (Jones), the detectivity for bottom side irradiation: D_B =1.71 × 10^{16} Jones, where J_d is the dark current density. The quasi-linear *I-V* characteristics of the ZnO nanostructure photodetector were observed under dark conditions, and the ohmic contact formed between nanoparticles and the homoepitaxial nanowires was used to gain high detectivity of the photoconductors.[23] Actually the nonlinear *I-V* characteristics with nonsymmetric curve at voltages below ±1.5V, as shown in Fig.4e, which demonstrates certain electric potential actually existed in the ZnO nanostructural photodetector. Further experimental results prove that the bending of a single ZnO microwire by an external force could cause transformation of the I-V characteristics from linear to non-linear considering the piezoelectric effect, experimental results and theoritical simulation demonstrate non-linear I-V characteristic could be due to piezoelectric effect resulted electric potential as shown in Fig. 4(f-i), and the asymmetric change of the I-V curve under certain bias in our case is

dominated by the piezoelectric effect for the ZnO microwire, which tends to shift the height of the local interface barrier at the metal-ZnO contact, while photoexcitation using a light that has energy higher than the band gap of ZnO the barrier height could be tunned by piezophototronic effects. [40] Also, the photoresponse mechanisms for the ZnO material are commonly explained on the basis of the surface absorption and desorption of oxygen on the nanostructure. Because oxygen molecules are easily adsorbed onto the oxide surface because of the surface traps, the free electrons can be captured by the adsorption of oxygen to generate electronegative oxygen; a low-conductivity layer is then formed near the surface. Upon illumination with photons with energies greater than the bandgap of ZnO, photogenerated carriers are generated. The holes can be trapped near the semiconductor surface by the adsorbed electronegative oxygen. This hole-trapping mechanism through oxygen adsorption and desorption in ZnO is affected by the density of trap states formed by the dangling bonds on the nanostructure surface. Any detrimental recombination that occurs at the surface will reduce the magnitude of the photocurrent. Combining the effects such as photon trapping, surface plasmon resonance and piezophototronic effects together for the modulating carrier transport. The combination of the low dark current and large gain of the photoresponse is expected to yield a type of photodetector with the capability of a photodetector to detect the much weaker light signal.[14]

Given the photoresponse mechanisms of the self-bending assembled ZnO nanowire photodetector, surface-charge recombination is a possible mechanism for the narrow spectral photoresponse because of the numerous surface/interface-related phenomena observed in the nanostructures. Because the high-density dangling bonds and quick charge recombination allocated to the nanostructure surface enhanced visible photoluminescence emission,[45] high densities of surface charge traps were observed in ZnO nanostructures, which explains the large

photoconductive gain in ZnO photodetectors. Actually, the solution processed ZnO nanowires are unlikely to be free of surface defects. The surfaces will be contaminated through the attachment of the nonstoichiometric precursors when the nanowires are removed from the precursor solution. An unavoidable surface-charge recombination, especially for the self-bending assembled ZnO nanostrucutre photodetector, as shown in Fig.S7, strong UV emission located at ~380 nm (near band gap recombination) accompanied with non-negligible visible emission around 550 nm (surface-charge related recombination) could be clearly observed, which may be considered as one of the key factors enabling narrowband photodetection. It is also noted that the bandgap of ZnO could be modified under local-strain, which could induce light emission changes as reported by Zhi-min Liao et al. [46-48] Through comparing PL emissions of bending and free standing state nanowires, enhanced UV emission accompanied with slight peak shift was observed for bending state nanowires, here, crystal symmetry modification for contributing luminescence changes under strains is one of the influence factors. Because of the very large absorption coefficient of the ZnO nanowire materials with photon energies greater than the bandgap, the light penetration depth was very small (<370 nm); thus, most of the charge carriers were generated in a narrow region near the electrode, as illustrated in the irradiation-location-dependent photocurrent spectra. Under the above-bandgap photoexcitation, the generated charge carriers can be quenched easily because of the severe surface-charge recombination. Surface recombination may dominate the shorter UV photoresponse for the ZnO nanostructure detector.[49] In addition, the surface-charge sinks can quickly trap photogenerated charge carriers near the nanostructure surface. The shorter-UV-wavelength photoresponse inhibition is therefore supported because of the surface charge carrier recombination. Photons with energy approaching the bandgap energy penetrate much deeper because of their much higher absorption coefficient.

Under the external electric field, these photogenerated charge carriers are driven toward the electrode before recombination; thus, charge collection efficiency is increased. Therefore, a stronger photoresponse signal in the longer-UV-wavelength range is realized, resulting in the observed peak in the photocurrent spectra. However, with increasing electrical field strength, the charge extraction efficiency was further improved, and the photocurrent for the shorter UV wavelength range increased much more rapidly. This type of photodetector device lost its narrowband detection capability under an electrical field greater than 300 V/cm. A larger electric field quickly pushes the photogenerated carriers away from the surfaces, contributing to the generation of photocurrent before recombination. The photocurrent variation induced by a changing electric field can again be explained by the presence of the surface modification. However, the applied electric field should not be too large for narrowband photodetection.[45] The nanocrystal particle interfaces between the crystalline domains that make up the semiconductor photodetector are also critical for efficient charge transport control.[7] Transport within these domains, as well as at their boundaries, requires attention and optimization.[29] When interface barriers are formed among ZnO nanocrystal particle interfaces under irradiation with photon energies larger than the band gap, electrons in the valence band of ZnO are excited into the conduction band and strong local electric fields are formed in the depletion region,[40] the current is generated only when these photogenerated charge carriers can drift or diffuse to the electrode before recombination. Under light irradiation at the depletion region or at a location less than a diffusion length away, the photogenerated electrons and holes are quickly swept away in opposite directions by the strong local electric field. Therefore, the local conductance is greatly enhanced, followed by a depressed recombination rate. The local net charge density is decreased with the migration of the photogenerated carriers in the depletion layer, and the local electric

field is diminished. In addition, the factors such as the vacuum, temperature and humidity should also be considered for the photoresponse signal contribution, which may cause adsorbtion/desorption of environmental molecules on the nanostructure surfaces, or affect carrier transport properties, resulting in changes for photoresponse behaviors. And in our measurment process, all the experiments were carried out under constant ambient conditions, these aformentioned influences are much weaker from one or another photodetectors.

To evaluate overall performance of the designed ZnO nanowire UV photodetectors, responsitivity spectra measurements were carried out while changing corresponding parameters such as: irradiation photoactive layers, Au modification, distance, electrical field and nanowire standing state, corelations could be clearly made for carifying specialities for the constructed UV detectors compared with generally built ones as shown in Fig.5(a-g). Through carefully checking responsivity spectra of the ZnO nanostructure photodetector while varying corresponding parameters, photon-alternative detection or response output signal intensity could be well modulated through surface/interface carrier transport control. Here, in order to compare differentials of the device under different conditions, the photoresponsivity difference Δ_R was designed as:

$$\Delta_R = R_{\max,\lambda} - R_{\min,\lambda}, \qquad 5)$$

where $R_{\max,\lambda}$ and $R_{\min,\lambda}$ represents maximum and minmum responsitivity under certain wavelength for the detectors. Through overall measurement of the designed detectors, it could be concluded as following: 1) as shown in Fig.5(a,b), more than 3 orders enhancement for Δ_R could be realized in the spectra ranging from 325 to 350 nm after Au modification based on self-bending assembled ZnO nanowire photodetector, which demonstrate an ultra-high specific ratio

as a photonalternaive detector; 2) only responsitivity enhancement (more than 2 orders) located around 380 nm was observed without modifying alphabet of lines for the spectra (Fig.5c,d); 3) in accordance with literature results, higher responsitivity could be realized by varying irradiation distance or larger electric filed, which proves that photogenerated carriers could be efficiently collected before recombination in the region less than the diffusion length or under larger electric field,[21,42] and shorter UV wavelength response can be recoverd; 4) through comparing responsitivity of the nanowire photodetectors by utilizing vertically aligned or self-bending states, responsivity enhanced (more than 2 orders) could be clearly observed. Meanwhile, the photonresponse speed is commonly measured as a dominant parameter for practical applications, under a chopper-generated short-light-pulse signal, the response time of the designed ZnO nanostructure photodetectors could be applied for repeated measurement, and a fast and a slow recovery processes of 0.27 ms and 4.52 ms for nanowire device could be realized as shown in Fig.5(h,i), respectively. The self-bending-assembled ZnO nanowires modified with Au nanoparticles with very high carrier mobility increase the effective difussion and dominated the rapid recovery rate, and the surface/interface states in the ZnO nanostructures contributes a key role for the slow process. [25] At present, none of the articles have fully explored the detailed mechanisms of the UV photodetectors based on self-bending assembled ZnO nanowires which could be well modulated as discussed in above, only a few research papers have reported narrowband photoresponse behavior based on the built structure, here, in order to compare speciality differences with others, only a few literatures related with photodetectors owning narrowband response behaviors were cited as shown in Table 1 by comparing the parameters of the present and previous reported ones, it could be clearly observed that the built device owning ultrahigh detectivity and modulated photoresponse behavior could be realized under ultralow

bias of 0.2 V. As such, a kind of UV photodetector with modulated photoresponse could be realized through surface/interface carrier transport control, and excellent performance of ultrahigh detectivity photodetector under ultralow bias with specific spectrum detection and fast response time could be constructed, which satisfies the practical needs for low power consumption, high sensitivity applications especially in the UV region.[14]

3. CONCLUSION

In conclusion, the designed device with detectivity as high as of 1.69×10^{16} / 1.71×10^{16} cm·Hz$^{1/2}$ /W irradiated with 380 nm photons under ultralow bias of 0.2 V by alternating photoactive layers was obtained with consideration of photon-trapping, surface plasmonic resonance, piezophototronic effect and energy band engineering, respectively. A kind of modulated UV photodetector was realized through surface/interface carrier transport control based on self-bending assembled ZnO nanowires. UV photodetection could be performed within narrowband under varying correlated key parameters, with respect to efficient carrier trapping or transport control, spectrally resolved photoresponses of the detector revealed photoselective detection in the ultraviolet region for contributing detected signal. It is believed that carriers could be efficiently controlled by the surface/interface states of the self-bending-assembled ZnO nanowires, and photon-alternative detection was allowed or limited by the photoactive layers, diffusion length, piezophototronic effects and electric field. Because of the efficient carrier trapping/transport among ZnO nanostructural devices, the carrier transport properties of these systems were strongly limited or allowed in the dark or UV photon irradiation. Therefore, the photoresponse of the selective wavelength band resulted from effective carrier generation, separation and transport, which could be effectively modulated through optimal structure design. The response time of the photodetector showed rise or decay time in the order of millisecond,

which satisfy the practical needs of such a device. Hence, a high-performance UV photodetector with both high sensitivity and quick response speed is realized through modulation of the contribution of the surface/interface carrier transport mechanisms. More importantly, the idea of exploration of the constructed device in the paper could also be applied for designing photoelectric devices especially in nano research filed considering surface/interface carrier transport properties in the visible or infrared region with improved performace.

4. EXPERIMENTAL METHODS

Material preparation:

For ZnO nanowires: firstly the ZnO nanoparticle films were prepared by radio-frequency (RF) magnetron sputtering method using a 99.999% pure ZnO target. Before being loaded into the sputtering chamber, the quartz glass substrate was cleaned by organic solvents, sulfuric acid hydrogen peroxide mixture and rinsed by deionized water to remove the contaminations. During the sputtering process, a mixed gas of oxygen and argon with the same flow rate of 20 standard cubic centimeters per minute (SCCM) was introduced into the chamber and the working pressure was maintained at 1 Pa. The substrate was kept at room temperature with a rotation speed of 20 loops per minute. Nanoparticle size of the supporting seed layers could be tuned by post annealing process, growth time and buffer layers. Then a solution process hydrothermal method was explored to grown homoepitaxial nanowires on ZnO nanoparticle film using $Zn(CH_3COO)_2 \cdot 2H_2O$ and $C_6H_{12}N_4$ as reactant source. The reaction solution was adjusted to identical concentration (0.01 mol /L). Then the reaction kettle was put into an oven and maintained at 90 °C. Finally, the obtained sample was rinsed by deionized water and dried in the oven. Standing states of the ZnO nanowires could be well tuned by exploring supporting seed layers or post-growth process exploring liquid solution.

For ZnO microwire with length up to several centemeters: a simple one-step chemical vapor deposition (CVD) method was carried out to prepare ZnO microwire using a furnace tube, using a mixture of ZnO and graphite powders with a weight ratio of 1 :1 as the reactant source material. A silicon substrate with a ZnO thin film as seed layer (deposited via a radio frequency magnetron sputtering method) was utilized as a target. The tube furnace was heated to 1200 °C at a rate of 25 °C per minute under a constant flow of Argon gas (160 standard cubic centimeters per minute) as the protecting gas. After being maintained at 1200 °C for 1h to until all the reaction was completed to obtain the microwire with length as long as possible, the furnace was cooled down to room temperature naturally. Then, the ZnO microwires with length up to several centemeters could be synthesized on the substrate.

Devices fabrication:

For ZnO nanowires photodetector: to make photodetectors, PMMA resist was used as an insulating transparent filling material for the interspace of the free-standing or bending states nanowires, and oxygen plasma was explored to make the tops of the nanowires uncovered for metal electrods preparation, then a sencond time oxygen plasma was applied to make the surfaces of the ZnO nanowires fully uncovered by PMMA resist. In metal electrodes on the tops of ZnO nanowires were explored as Ohmic contacts. Here, the homo-epitaxial quasi-single crystal ZnO nanowires could be regarded both as photoactive layers and vertical electrodes for the photodetectors due to ultra-high diffusion length more than 100 μm. The surfaces of the obtained nanowires could be modified by partial coverage of the metal nanoparticles for enhancing the performances of the photodetectors. Here, gold nanoparticles were deposited on the surface of the ZnO nanowires for metal modification using an ion-sputtering method.

For single ZnO microwire device: To fabricate single microwire device applied for piezoelectric effect measurement, a single ZnO microwire with length up to 3 cm was selected. Both ends of the microwire were contacted with In metal deposited on flexible PET substrate as electrodes. Bending experiments of single microwire device could be carried out by external force using mechnical displacement fixture with minmum precision of ± 0.5 μm.

Appratus Applied:

SEM images were captured by Hitachi S-4800, PL measurement was measured using a JY-630 micro-Raman spectrometer with the 325 nm line of He–Cd laser as excitation source. The photocurrent spectra of the devices were detected by a standard lock-in technique with a 150 W Xe lamp as an excitation light source. Current versus voltage (I-V) measurement was performed by a Lakeshore 7707 Hall measurement system. The UV-Vis absorption spectra were recorded on a PerkinElmer Lamda950 spectrophotometer. X-ray diffraction (XRD) was performed using a Bruker Advance D8 X-ray diffractometer. Transmission electron microscopy (TEM) measurements were performed with an FEI Tecnai G220 instrument.

FIGURES

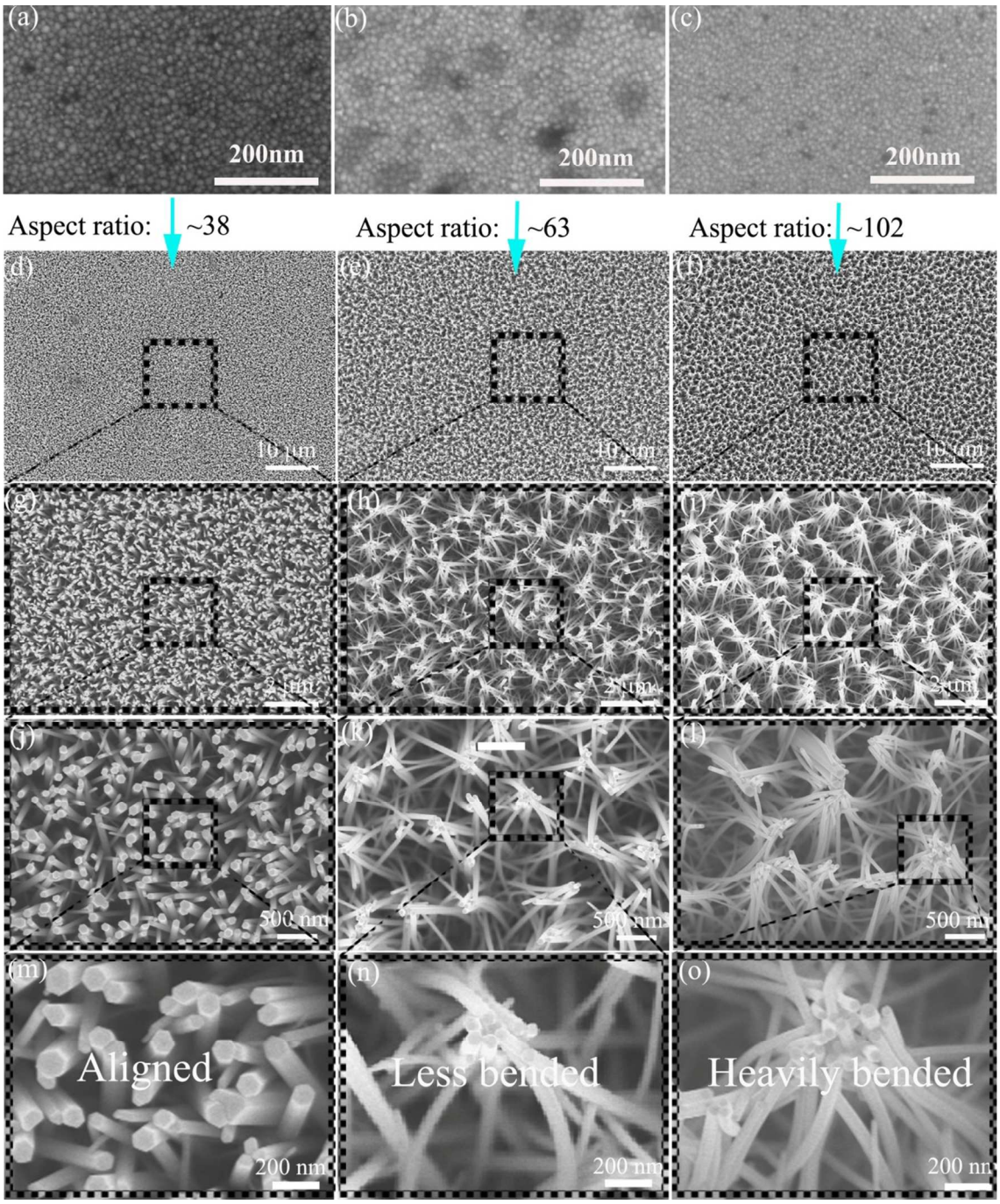

Figure 1. SEM images of non bended, less bended and heavily bended ZnO nanowires. (a-c) SEM images of ZnO nanoparticles. (d-o) SEM images of self-assembled ZnO nanowires with free standing state, the tops of the nanowires display hexagnol morphology with non bended state, SEM images of ZnO nanowires with less bended state, the average amount of the nanowires agglomerated together is ~10, SEM images of ZnO nanowires with heavily bended state, the average amount of the nanowires agglomerated together can be ~ 20, respectively.

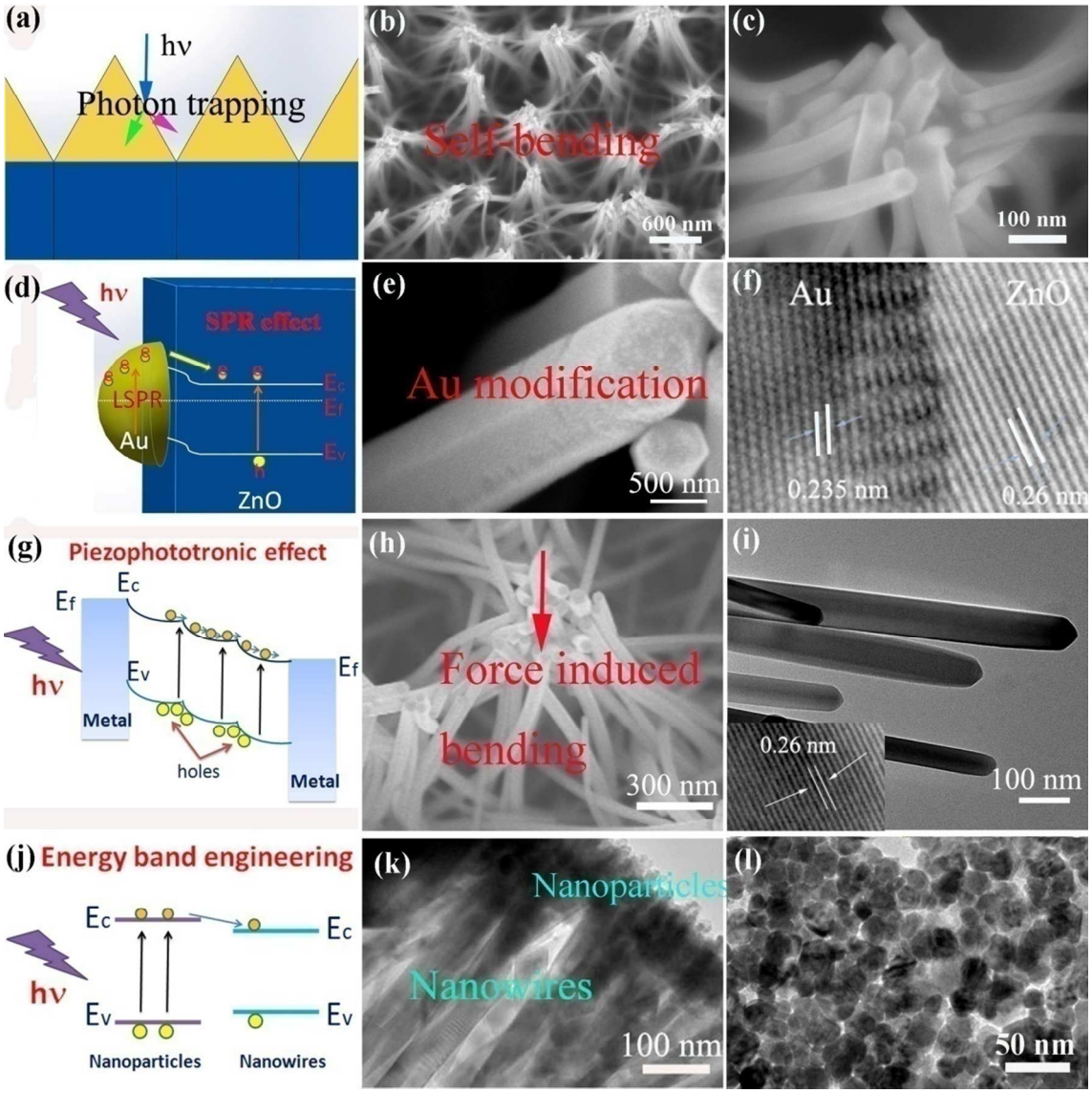

Figure 2. Ultraviolet photodetector designed by considering the dominant factors such as structure, surface modification, piezophototronic effects and energy band engineering. (a) schematic diagram of photon trapping in pyramid structure, (b,c) SEM image of self-assembled ZnO nanowires with tops agglomerated structure, which mimics typical conventional pyramide structure for efficient photon trapping. (d) schematic diagram of surface plasmon resonance between Au and ZnO, (e,f) SEM and HRTEM images of ZnO nanowires functionalized with plasmonic Au nanoparticles, (g) schematic band structure diagram of ZnO material considering piezophototronic effect. (h) SEM image of self-bending assembled single bound ZnO nanowires. (i) TEM and HRTEM images of the ZnO nanowires. (j) schematic energy band diagram of ZnO

nanowires and nanoparticles, through UV photon excitation, the generated carriers in nanoparticles could be easily diffused into nanowires, (k,l) TEM images of ZnO nanowires and nanoparticles.

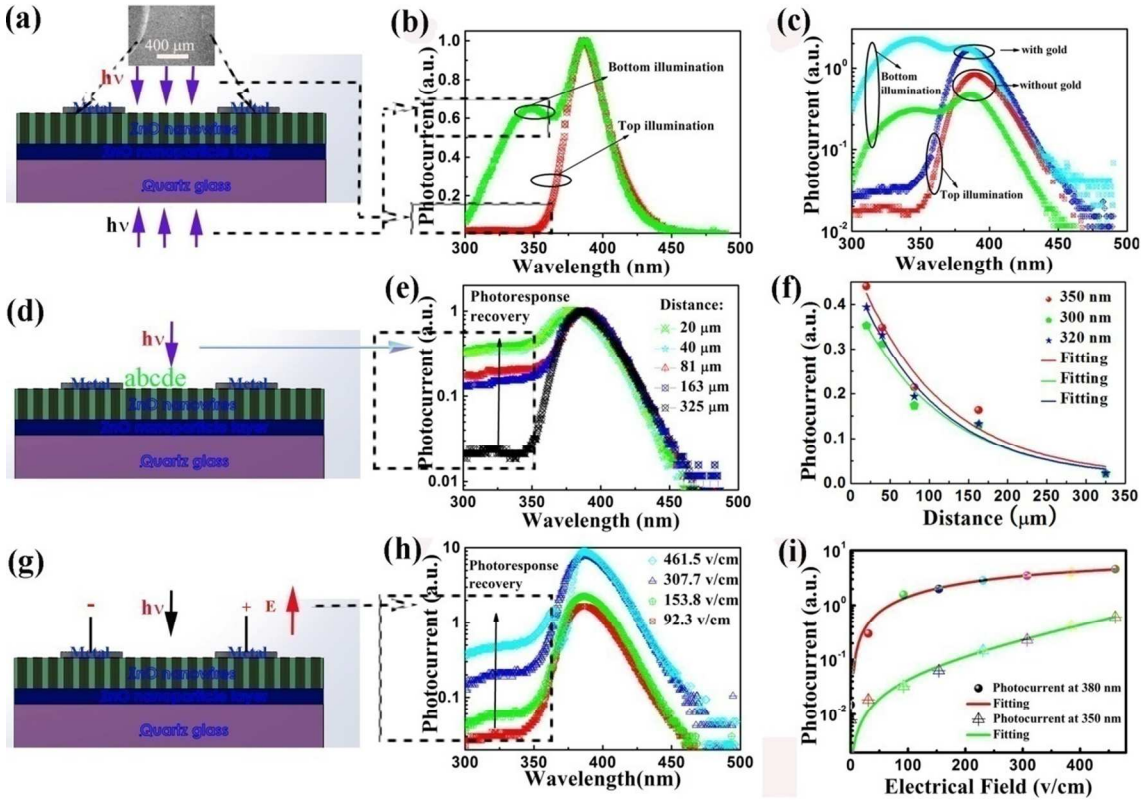

Figure 3. Alternative UV photondetection of ZnO detectors measured while changing irradiation photoactive layers, distance from one of the electrodes and electrical field for exploring photonresponse mechanisms based on as grown and Au nanoparticle modified ZnO nanowires devices. (a,d,g) schematic diagrams of ZnO nanostructure photodetector under UV light irradiation on the surface of ZnO nanowires or quartz glass side, respectively, (b,c) photoresponse spectra of self-bending assembled ZnO photodetectors irradiated from corresponding locations, experimental results demonstrate increased photocurrent was realized after Au modification, (e,f) photocurrent spectra and analytical fitting results of ZnO photodetectors demonstrate exponential decay with increasing distance, (h,i) photocurrent spectra and analytical fitting results of the obtained data located at 350, 380 nm, respectively demonstrate exponential growth with increasing electrical field.

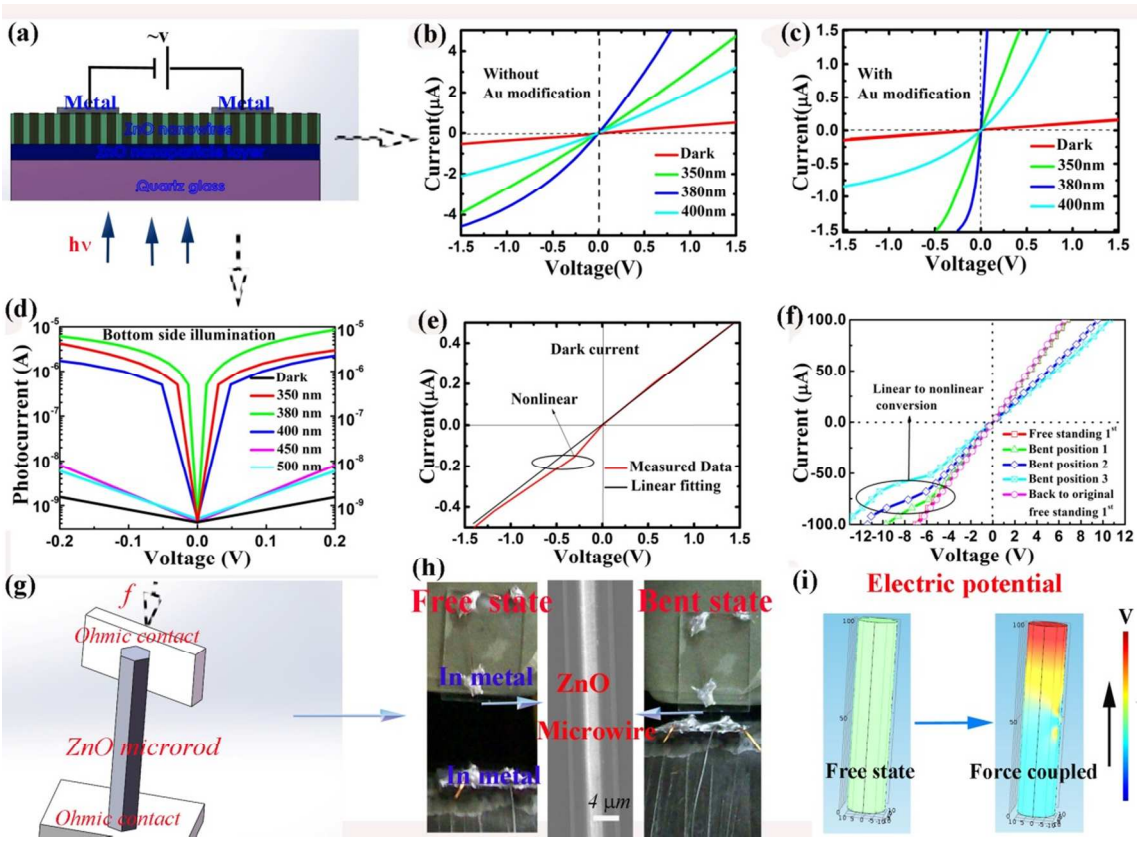

Figure4. Current-voltage characteristics of ZnO nanostructure photodetectors explored with and without Au modification, applying force induced bending and by changing irradiation location. (a) schematic diagram of ZnO photodetector, (b,c) I-V characteristics of the photodetectors without and with gold modification under dark and different irradiation of 350, 380 and 400 nm from bottom side, (d) represent I-V characteristic of the self-bending assembled ZnO nanowire photodetectors under dark and different illumination wavelengths of 350, 380 and 400, 450, 500 nm from top and bottom side, respectively, (e) dark current measurement for self-bending assembled ZnO nanowire photodetector, (e,f) I-V characteristic of single ZnO microrod with In metal electrodes under free-standing or bending states, nonlinear phonenom occured under bending state considering piezoelectric effect. The *I-V* characteristics of the ZnO microrod in the free standing (from the free standing 1st to 2nd indicate the initial and the final free standing states of the ZnO microrod) or different bending states (from bent position 1 to 3 indicate the increase of the bending) (g) schematic diagram of single ZnO microrod coupling with force, (h) experimental set-up single ZnO microrod under free or bent state, (i) electric potential distribution of single ZnO microrod under free or bent state through theoretical simulation

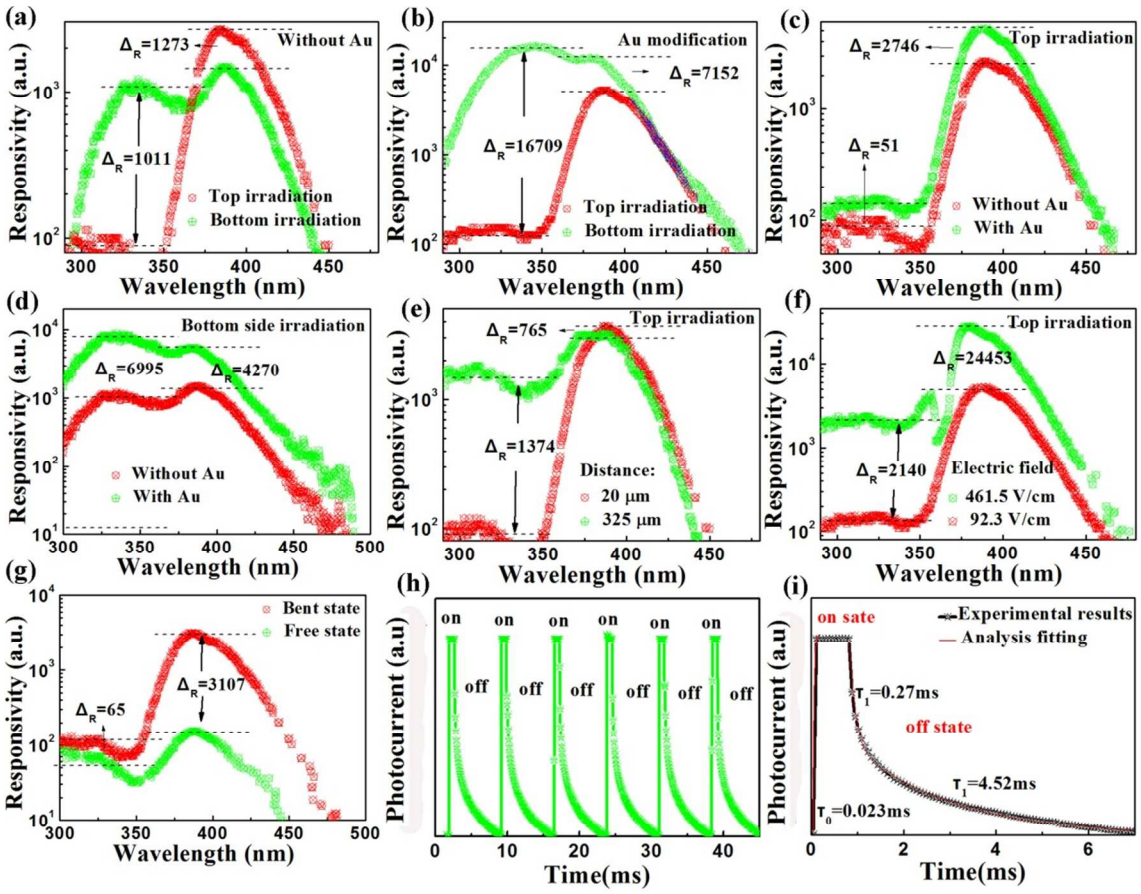

Figure 5. Performance evaluation of the designed ZnO UV photodetectors while changing corresponding parameters such as: irradiation photoactive layers, Au modification, distance, electrical field and nanowire standing state, which shows corelations for the ZnO nanowires devices. (a-g) responsivity spectra of ZnO nanostructure photodetector while varying corresponding parameters, respectively, (h,i) Time-resolved photocurrent of the designed self-bending assembled ZnO nanowire photodetectors under UV on and off states.

TABLES

Table 1. Comparison of the alphabet of lines, detectivity, dark current, recovery time between present photodetectors and previous reported ones.

Photodetectors	**Response Type**	**Detectivity** (Jones)	**Dark Current**	**Recovery Time**	**Ref. No.**
ZnO nanowire	Non photon-alternative	3.3×10^{17} (1V, 365 nm)	20 pA	0.32 s	[21]
Colloidal ZnO Nanoparticles	Non photon-alternative	~	(<120 pA) /120V	1 s	[15]
graphene–quantum dot	Non photon-alternative	7×10^{13}	~	~	[50]
perovskite single-crystal	Non photon-alternative	2×10^{10} (570 nm)	~nA	~ms	[45]
n-ZnO/p-NiO core–shell nanowire	Non photon-alternative	~	~	10.0 μs and 30.3 μs	[51]
Self-bending assembled ZnO nanowires	Photon-alternative	1.69×10^{16} /1.7×10^{16} (0.2V, 380 nm)	~1 nA (0.2V)	Growth:0.023 ms, decay1:0.47 ms; decay2: 4.52 ms	Present work

Supporting Information.

Schematic diagram of the ZnO nanowire photodetector； ZnO nanostructure photodetector fabrication processess； Absorption spectra ZnO structure； Schematic diagram and SEM image of pyramid strucutre; Scehmatic diagram of ZnO with and without gold modification in the dark, under UV light on and off states; Photocurrent spectra of ZnO detectors utilizing nanowires with vertically aligned or self-bending assmbled structure; PL spectra of bending and free standing state ZnO nanowires; Mechanism of narrowband photodetection.

The supporting figures in the paper could be obtained in the supporting information file, and this information is available free of charge via the Internet at http://pubs.acs.org/.

AUTHOR INFORMATION

Corresponding Author

*Zhen Guo. Key Lab of Bio-Medical Diagnostics, Suzhou Institute of Biomedical Engineering and Technology, Chinese Academy of Sciences. No.88, Keling Road, Suzhou New District, 215163, People's Republic of China. E-mail: guozhen@sibet.ac.cn;

*Dongxu Zhao. The State Key Laboratory of Luminescence and Applications, Changchun Institute of Optics, Fine Mechanics and Physics, Chinese Academy of Sciences, 3888 East Nan-Hu Road, Open Economic Zone, Changchun 130033, People's Republic of China. E-mail: zhaodx@ciomp.ac.cn;

Author Contributions

The manuscript was written through contributions of all authors. All authors have given approval to the final version of the manuscript.

ACKNOWLEDGMENT

This work is supported by the National Natural Science Foundation of China under Grant Nos.(51202154, 51675517, 51205268), the Natural Science Foundation of Jiangsu Province under Grant Nos.(BK2013116, BK20160057, BK2012190) and Major Technology Innovation Projects of Jiangsu Province (No. BO2015007)，the Key Research Program of the Chinese Academy of Sciences，Grant NO：KFZD-SW-204, National Key Instrument Developing Project of China under Grant No. ZDYZ2013-1, the SRF for ROCS, SEM, and the Project funded by China Postdoctoral Science Foundation under Grant No. 2016M601890”

REFERENCES AND NOTES

(1) Simon, J.; Protasenko, V.; Lian, C. X.; Xing, H. L.; Jena, D. Polarization-Induced Hole Doping in Wide-Band-Gap Uniaxial Semiconductor Heterostructures. *Science* **2010**, *327*, 60-64.

(2) Uoyama, H.; Goushi, K.; Shizu, K.; Nomura, H.; Adachi, C. Highly Efficient Organic Light-Emitting Diodes from Delayed Fluorescence. *Nature* **2012**, *492*, 234-238.

(3) Shi, D.; Adinolfi, V.; Comin, R.; Yuan, M. J.; Alarousu, E.; Buin, A.; Chen, Y.; Hoogland, S.; Rothenberger, A.; Katsiev, K.; Losovyj, Y.; Zhang, X.; Dowben, P. A.; Mohammed, O. F.; Sargent, E. H.; Bakr, O. M. Low Trap-State Density and Long Carrier Diffusion in Organolead Trihalide Perovskite Single Crystals. *Science* **2015**, *347*, 519-522.

(4) Xing, G. C.; Mathews, N.; Sun, S. Y.; Lim, S. S.; Lam, Y. M.; Gratzel, M.; Mhaisalkar, S.; Sum, T. C. Long-Range Balanced Electron- and Hole-Transport Lengths in Organic-Inorganic Ch3nh3pbi3. *Science* **2013**, *342*, 344-347.

(5) Polman, A.; Knight, M.; Garnett, E. C.; Ehrler, B.; Sinke, W. C. Photovoltaic Materials: Present Efficiencies and Future Challenges. *Science* **2016**, *352*, aad4424(1-10).

(6) Hwang, Y. J.; Hahn, C.; Liu, B.; Yang, P. D. Photoelectrochemical Properties of TiO2 Nanowire Arrays: A Study of the Dependence on Length and Atomic Layer Deposition Coating. *Acs Nano* **2012**, *6*, 5060-5069.

(7) Graetzel, M.; Janssen, R. A. J.; Mitzi, D. B.; Sargent, E. H. Materials Interface Engineering for Solution-processed Photovoltaics. *Nature* **2012**, *488*, 304-312.

(8) Nakano, M.; Shibuya, K.; Okuyama, D.; Hatano, T.; Ono, S.; Kawasaki, M.; Iwasa, Y.; Tokura, Y. Collective Bulk Carrier Delocalization Driven by Electrostatic Surface Charge Accumulation. *Nature* **2012**, *487*, 459-462.

(9) Fu, X. W.; Liao, Z. M.; Xu, J.; Wu, X. S.; Guo, W. L.; Yu, D. P. Improvement of Ultraviolet Photoresponse of Bent ZnO Microwires by Coupling Piezoelectric and Surface Oxygen Adsorption/Desorption Effects. *Nanoscale* **2013**, *5*, 916-920.

(10) Tsang, M. K.; Bai, G. X.; Hao, J. H. Stimuli Responsive Upconversion Luminescence Nanomaterials and Films for Various Applications. *Chem Soc Rev* **2015**, *44*, 1585-1607.

(11) Wan, D. H.; Chen, H. L.; Tseng, T. C.; Fang, C. Y.; Lai, Y. S.; Yeh, F. Y. Antireflective Nanoparticle Arrays Enhance the Efficiency of Silicon Solar Cells. *Adv Funct Mater* **2010**, *20*, 3064-3075.

(12) McCold, C. E.; Fu, Q.; Howe, J. Y.; Hihath, J. Conductance Based Characterization of Structure and Hopping Site Density in 2d Molecule-Nanoparticle Arrays. *Nanoscale* **2015**, *7*, 14937-14945.

(13) Li, K. Y.; Shan, Q. S.; Zhu, R. P.; Yin, H.; Lin, Y. Y.; Wang, L. Q. Carrier Transport in Quantum Dot Quantum Well Microstructures of the Self-Assembled Cdte/Cds/Ligand Core-Shell System. *Nanoscale* **2015**, *7*, 7906-7914.

(14) Guo, F. W.; Yang, B.; Yuan, Y. B.; Xiao, Z. G.; Dong, Q. F.; Bi, Y.; Huang, J. S. A Nanocomposite Ultraviolet Photodetector Based on Interfacial Trap-Controlled Charge Injection. *Nat Nanotechnol* **2012**, *7*, 798-802.

(15) Jin, Y. Z.; Wang, J. P.; Sun, B. Q.; Blakesley, J. C.; Greenham, N. C. Solution-Processed Ultraviolet Photodetedtors Based on Colloidal ZnO Nanoparticles. *Nano Lett* **2008**, *8*, 1649-1653.

(16) Konstantatos, G.; Howard, I.; Fischer, A.; Hoogland, S.; Clifford, J.; Klem, E.; Levina, L.; Sargent, E. H. Ultrasensitive Solution-Cast Quantum Dot Photodetectors. *Nature* **2006**, *442*, 180-183.

(17) Konstantatos, G.; Sargent, E. H. Nanostructured Materials for Photon Detection. *Nat Nanotechnol* **2010**, *5*, 391-400.

(18) Seong, H.; Yun, J.; Jun, J. H.; Cho, K.; Kim, S. The Transfer of Charge Carriers Photogenerated in ZnO Nanoparticles into a Single ZnO Nanowire. *Nanotechnology* **2009**, *20,*245201.

(19) Hochbaum, A. I.; Yang, P. D. Semiconductor Nanowires for Energy Conversion. *Chem Rev* **2010**, *110*, 527-546.

(20) Dong, Q. F.; Fang, Y. J.; Shao, Y. C.; Mulligan, P.; Qiu, J.; Cao, L.; Huang, J. S. Electron-Hole Diffusion Lengths > 175 μm in Solution-Grown Ch3nh3pbi3 Single Crystals. *Science* **2015**, *347*, 967-970.

(21) Liu, X.; Gu, L. L.; Zhang, Q. P.; Wu, J. Y.; Long, Y. Z.; Fan, Z. Y. All-Printable Band-Edge Modulated ZnO Nanowire Photodetectors with Ultra-High Detectivity. *Nat Commun* **2014**, *5,*4007-4015.

(22) Li, Y. B.; Della Valle, F.; Simonnet, M.; Yamada, I.; Delaunay, J. J. High-Performance UV Detector Made of Ultra-Long ZnO Bridging Nanowires. *Nanotechnology* **2009**, *20,*045501-045505.

(23) Soci, C.; Zhang, A.; Xiang, B.; Dayeh, S. A.; Aplin, D. P. R.; Park, J.; Bao, X. Y.; Lo, Y. H.; Wang, D. ZnO Nanowire UV Photodetectors with High Internal Gain. *Nano Lett* **2007**, *7*, 1003-1009.

(24) Lao, C. S.; Park, M. C.; Kuang, Q.; Deng, Y. L.; Sood, A. K.; Polla, D. L.; Wang, Z. L. Giant Enhancement in UV Response of ZnO Nanobelts by Polymer Surface-Functionalization. *J Am Chem Soc* **2007**, *129*, 12096-12097.

(25) Liu, K. W.; Sakurai, M.; Aono, M.; Shen, D. Z. Ultrahigh-Gain Single Sno2 Microrod Photoconductor on Flexible Substrate with Fast Recovery Speed. *Adv Funct Mater* **2015**, *25*, 3157-3163.

(26) Wang, H. B.; Gonzaez-Pedro, V.; Kubo, T.; Fabregat-Santiago, F.; Bisquert, J.; Sanehira, Y.; Nakazaki, J.; Segawa, H. Enhanced Carrier Transport Distance in Colloidal Pbs Quantum-Dot-Based Solar Cells Using ZnO Nanowires. *J Phys Chem C* **2015**, *119*, 27265-27274.

(27) Gao, Y.; Wang, Z. L. Equilibrium Potential of Free Charge Carriers in a Bent Piezoelectric Semiconductive Nanowire. *Nano Lett* **2009**, *9*, 1103-1110.

(28) Valdez, C. N.; Schimpf, A. M.; Gamelin, D. R.; Mayer, J. M. Proton-Controlled Reduction of ZnO Nanocrystals: Effects of Molecular Reductants, Cations, and Thermodynamic Limitations. *J Am Chem Soc* **2016**, *138*, 1377-1385.

(29) Lee, Y. J.; Ruby, D. S.; Peters, D. W.; McKenzie, B. B.; Hsu, J. W. P. ZnO Nanostructures as Efficient Antireflection Layers in Solar Cells. *Nano Lett* **2008**, *8*, 1501-1505.

(30) Atwater, H. A.; Polman, A. Plasmonics for Improved Photovoltaic Devices. *Nat Mater* **2010**, *9*, 205-213.

(31) Liu, K. W.; Sakurai, M.; Liao, M. Y.; Aono, M. Giant Improvement of the Performance of ZnO Nanowire Photodetectors by Au Nanoparticles. *J Phys Chem C* **2010**, *114*, 19835-19839.

(32) Gogurla, N.; Sinha, A. K.; Santra, S.; Manna, S.; Ray, S. K. Multifunctional Au-ZnO Plasmonic Nanostructures for Enhanced UV Photodetector and Room Temperature NO Sensing Devices. *Sci Rep-Uk* **2014**, *4,* 6483-6411.

(33) Wang, Z. L.; Wu, W. Z. Piezotronics and Piezo-phototronics: Fundamentals and Applications. *Natl Sci Rev* **2014**, *1*, 62-90.

(34) Liu, Y.; Zhang, Y.; Yang, Q.; Niu, S. M.; Wang, Z. L. Fundamental Theories of Piezotronics and Piezo-phototronics. *Nano Energy* **2015**, *14*, 257-275.

(35) Wu, W. Z.; Pan, C. F.; Zhang, Y.; Wen, X. N.; Wang, Z. L. Piezotronics and Piezo-phototronics - From Single Nanodevices to Array of Devices and Then to Integrated Functional System. *Nano Today* **2013**, *8*, 619-642.

(36) Mandalapu, L. J.; Yang, Z.; Xiu, F. X.; Zhao, D. T.; Liu, J. L. Homojunction Photodiodes based on Sb-doped P-type ZnO for Ultraviolet Detection. *Appl Phys Lett* **2006**, *88,*383-385.

(37) Ni, P. N.; Shan, C. X.; Wang, S. P.; Li, B. H.; Zhang, Z. Z.; Zhao, D. X.; Liu, L.; Shen, D. Z. Enhanced Responsivity of Highly Spectrum-Selective Ultraviolet Photodetectors. *J Phys Chem C* **2012**, *116*, 1350-1353.

(38) Kim, J.; Yun, J. H.; Kim, C. H.; Park, Y. C.; Woo, J. Y.; Park, J.; Lee, J. H.; Yi, J.; Han, C. S. ZnO Nanowire-Embedded Schottky Diode for Effective Uv Detection by the Barrier Reduction Effect. *Nanotechnology* **2010**, *21,*115205-115209.

(39) Atwater, H. A.; Polman, A. Plasmonics for Improved Photovoltaic Devices (vol 9, pg 205, 2010). *Nat Mater* **2010**, *9*, 865-865.

(40) Hu, Y. F.; Chang, Y. L.; Fei, P.; Snyder, R. L.; Wang, Z. L. Designing the Electric Transport Characteristics of ZnO Micro/Nanowire Devices by Coupling Piezoelectric and Photoexcitation Effects. *Acs Nano* **2010**, *4*, 1234-1240.

(41) Zhu, L. H.; Gu, X. H.; Qu, F. D.; Zhang, J. Q.; Feng, C. H.; Zhou, J. R.; Ruan, S. P.; Kang, B. N. Electrospun ZnO Nanofibers-Based Ultraviolet Detector with High Responsivity. *J Am Ceram Soc* **2013**, *96*, 3183-3187.

(42) Yang, Q.; Guo, X.; Wang, W. H.; Zhang, Y.; Xu, S.; Lien, D. H.; Wang, Z. L. Enhancing Sensitivity of a Single ZnO Micro-/Nanowire Photodetector by Piezo-phototronic Effect. *Acs Nano* **2010**, *4*, 6285-6291.

(43) Harnack, O.; Pacholski, C.; Weller, H.; Yasuda, A.; Wessels, J. M. Rectifying Behavior of Electrically Aligned ZnO Nanorods. *Nano Lett* **2003**, *3*, 1097-1101.

(44) Lao, C. S.; Liu, J.; Gao, P. X.; Zhang, L. Y.; Davidovic, D.; Tummala, R.; Wang, Z. L. ZnO Nanobelt/nanowire Schottky Diodes Formed by Dielectrophoresis Alignment Across Au Electrodes. *Nano Lett* **2006**, *6*, 263-266.

(45) Fang, Y. J.; Dong, Q. F.; Shao, Y. C.; Yuan, Y. B.; Huang, J. S. Highly Narrowband Perovskite Single-Crystal Photodetectors Enabled by Surface-Charge Recombination. *Nat Photonics* **2015**, *9*, 679-686.

(46) Fu, X. W.; Li, C. Z.; Fang, L.; Liu, D. M.; Xu, J.; Yu, D. P.; Liao, Z. M. Strain-Gradient Modulated Exciton Emission in Bent ZnO Wires Probed by Cathodoluminescence. *Acs Nano* **2016**, *10*, 11469-11474.

(47) Fu, X. W.; Liao, Z. M.; Liu, R.; Lin, F.; Xu, J.; Zhu, R.; Zhong, W.; Liu, Y. K.; Guo, W. L.; Yu, D. P. Strain Loading Mode Dependent Bandgap Deformation Potential in ZnO Micro/Nanowires. *Acs Nano* **2015**, *9*, 11960-11967.

(48) Liao, Z. M.; Wu, H. C.; Fu, Q.; Fu, X. W.; Zhu, X. L.; Xu, J.; Shvets, I. V.; Zhang, Z. H.; Guo, W. L.; Leprince-Wang, Y. M.; Zhao, Q.; Wu, X. S.; Yu, D. P. Strain Induced Exciton Fine-Structure Splitting and Shift in Bent ZnO Microwires. *Sci Rep-Uk* **2012**, *2,*452-457.

(49) Guo, Z.; Zhao, D. X.; Liu, Y. C.; Shen, D. Z.; Zhang, J. Y.; Li, B. H. Visible and Ultraviolet Light Alternative Photodetector Based on ZnO Nanowire/N-Si Heterojunction. *Appl Phys Lett* **2008**, *93,*163501-163503.

(50) Konstantatos, G.; Badioli, M.; Gaudreau, L.; Osmond, J.; Bernechea, M.; de Arquer, F. P. G.; Gatti, F.; Koppens, F. H. L. Hybrid Graphene-Quantum Dot Phototransistors with Ultrahigh Gain. *Nat Nanotechnol* **2012**, *7*, 363-368.

(51) Ni, P. N.; Shan, C. X.; Wang, S. P.; Liu, X. Y.; Shen, D. Z. Self-Powered Spectrum-Selective Photodetectors Fabricated from N-Zno/P-Nio Core-Shell Nanowire Arrays. *J Mater Chem C* **2013**, *1*, 4445-4449.

TOC

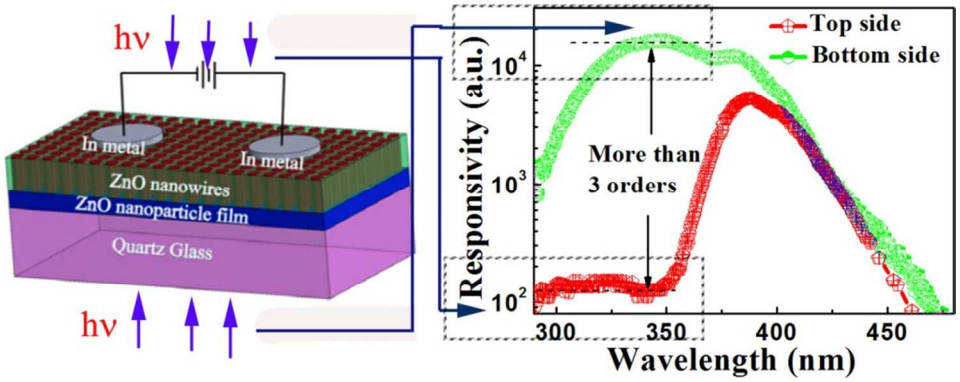
hν
In metal
In metal
ZnO nanowires
ZnO nanoparticle film
Quartz Glass
hν
Top side
Bottom side
Responsivity (a.u.)
10^4
10^3
10^2
More than
3 orders
300
350
400
450
Wavelength (nm)